Conformational Templates for Rational Drug Design: Flexibility of *cyclo*(D-Pro[1]-Ala[2]-Ala[3]-Ala[4]-Ala[5]) in DMSO Solution

Xiaoming Zhang, Gregory V. Nikiforovich,* and Garland R. Marshall

Department of Biochemistry and Molecular Biophysics, Washington University School of Medicine, 700 South Euclid Avenue, St. Louis, Missouri 63110

Received January 22, 2007

Long MD simulations (100 ns) for the important model cyclopentapeptide *cyclo*(D-Pro[1]-Ala[2]-Ala[3]-Ala[4]-Ala[5]) were performed in explicit DMSO solution using both OPLS-AA and AMBER03 force fields. Simulations revealed conformational transitions between two main conformers, a predominant one (population 93−99%) and a minor conformer (population 0.4−6.7%). These results are in excellent agreement with 20 experimental proton−proton distances estimated for this cyclopentapeptide. The previously discussed γ-turn-like conformation for Ala[4] was present only in a minor conformer.

Introduction

Because cyclic pentapeptides (CPPs[a]) presumably possess limited flexibility in solution, they may serve as convenient conformational templates for studies of ligand−receptor interaction in the rational design of pharmaceuticals. For instance, CPPs may mimic different types of β- and γ-turns, molecular scaffolds of choice in the search for drug candidates inhibiting protein/protein interactions.[1] CPPs can be readily synthesized, are resistant to proteases, and did not provoke immunogenic responses. Conformational features for many CPPs (mostly containing one or two D-amino acid residues) have been extensively studied by NMR measurements and X-ray spectroscopy (see, e.g., ref 2 and references therein).

General approaches proposed to determine 3D structure(s) of CPPs in solution included measuring NMR parameters (e.g., NOEs and vicinal constants) followed by molecular dynamics (MD) simulations employing the experimental NMR parameters as constraints.[3] For the important model compound *cyclo*(D-Pro[1]-Ala[2]-Ala[3]-Ala[4]-Ala[5]), pA_4, this approach yielded five different 3D structures in DMSO solution,[4] two of them containing a conformation close to the γ-turn for the backbone of Ala.[4] (The conformation of the γ-turn has been first determined as ϕ ca. 70°, ψ ca. −60°.[5]) Conformations with the positive ϕ and negative ψ values, such as the γ-turn, are usually considered as forbidden for L-amino acid residues, as well as conformations with negative ϕ and positive ψ values for D-amino acid residues (such as an inverse γ-turn, ϕ ca. −80°, ψ ca. 80°, which is allowed for L-amino acid residues). Indeed, the extensive review of experimental X-ray and NMR studies of 29 model CPPs reported backbone conformations of these types for only two chiral amino acid residues out of 110 indicating the unfavorable energetics of this conformation.[2] We have, therefore, previously suggested an alternative approach to study conformational flexibility of CPPs.[6] The approach estimates statistical weights for low-energy conformations of CPPs determined by independent energy calculations.[6] For pA_4, we have found that the experimental NMR parameters obtained in Mierke et al.[4] were consistent with averaging over five different low-energy structures, none of which contained the γ-turn-like conformation for a L-amino acid residues.[6] More recent structural studies of novel CPPs focused on antagonists of the CXCR4 receptor also did not report these type of conformations.[7]

Our previous calculations involved, however, some important limitations, such as employment of the ECEPP/2 force field featuring rigid valence geometry with planar nonproline peptide groups (i.e., the corresponding ω angles were fixed at 180°) and the absence of explicit solvent. Also, the very recent NMR study by Heller et al.[8] re-examined the conformational flexibility of pA_4 in DMSO solution using specific labeling of the backbone CO and NH groups with ^{13}C and ^{15}N, respectively.[8] This study found a minor conformer (15−30%) of pA_4 containing the γ-turn in question.[8] Our present communication reports the data from the much more thorough computational studies of pA_4 in DMSO solution.

Methods

The molecular dynamics simulations of pA_4 with explicit DMSO solvent molecules were performed using both the OPLS-AA and AMBER03 force field within the GROMACS 3.3 simulation package.[9] A cubic box of volume 2.44×10^4 Å^3 containing 198 DMSO molecules with periodic boundary conditions was used. The OPLS model used for the description of DMSO molecules employed the following set of parameters: r(C−S) = 1.80 Å, r(S−O) = 1.53 Å, σ_s = 3.56 Å, σ_o = 2.93 Å, σ_c = 3.81 Å, ϵ_s = 0.395 kcal/mol, ϵ_o = 0.280 kcal/mol, ϵ_c = 0.160 kcal/mol, q_s = 0.139 e, q_o = −0.459 e, and q_c = 0.160 e (parameters used previously by Zheng and Ornstein[10]). This model correctly reproduced the density and ΔH_{vap} for bulk DMSO at 300° K and 1 atm, as follows: density = 1107 kg/m^3 and ΔH_{vap} = 52.28 kJ/mol, the experimental values being 1095 kg/m^3 and 52.88 kJ/mol, respectively.[11] Energies of the solvated peptides were first minimized by 1000 steepest descent steps, and then simulated at 300° K and 1 atm using the constant temperature and pressure algorithm.[12] All MD simulations were performed with a time step of 1 fs and the atomic coordinates were saved every 10 000 steps. The PME algorithm with cutoffs of 13 Å for nonbonded interactions was used during the simulation.

Results and Discussion

Initial MD simulations were performed starting from 10 different conformations of pA_4 found as low-energy structures by preliminary energy calculations employing the ECEPP/2 force field, where all combinations of the local minima of the

* To whom correspondence should be addressed. Telephone: (314) 362-1566. Fax: (314) 362-0234. E-mail: gregory@ccb.wustl.edu.

[a] Abbreviations: CPP, cyclopentapeptide; NMR, nuclear magnetic resonance; NOE, nuclear Overhauser effect; MD, molecular dynamics; pA_4, *cyclo*(D-Pro[1]-Ala[2]-Ala[3]-Ala[4]-Ala[5]); ECEPP, OPLS-AA, and AMBER03, acronyms for force fields.

10.1021/jm070084n CCC: $37.00
Published on Web 05/11/2007 PAGE EST: 4.3

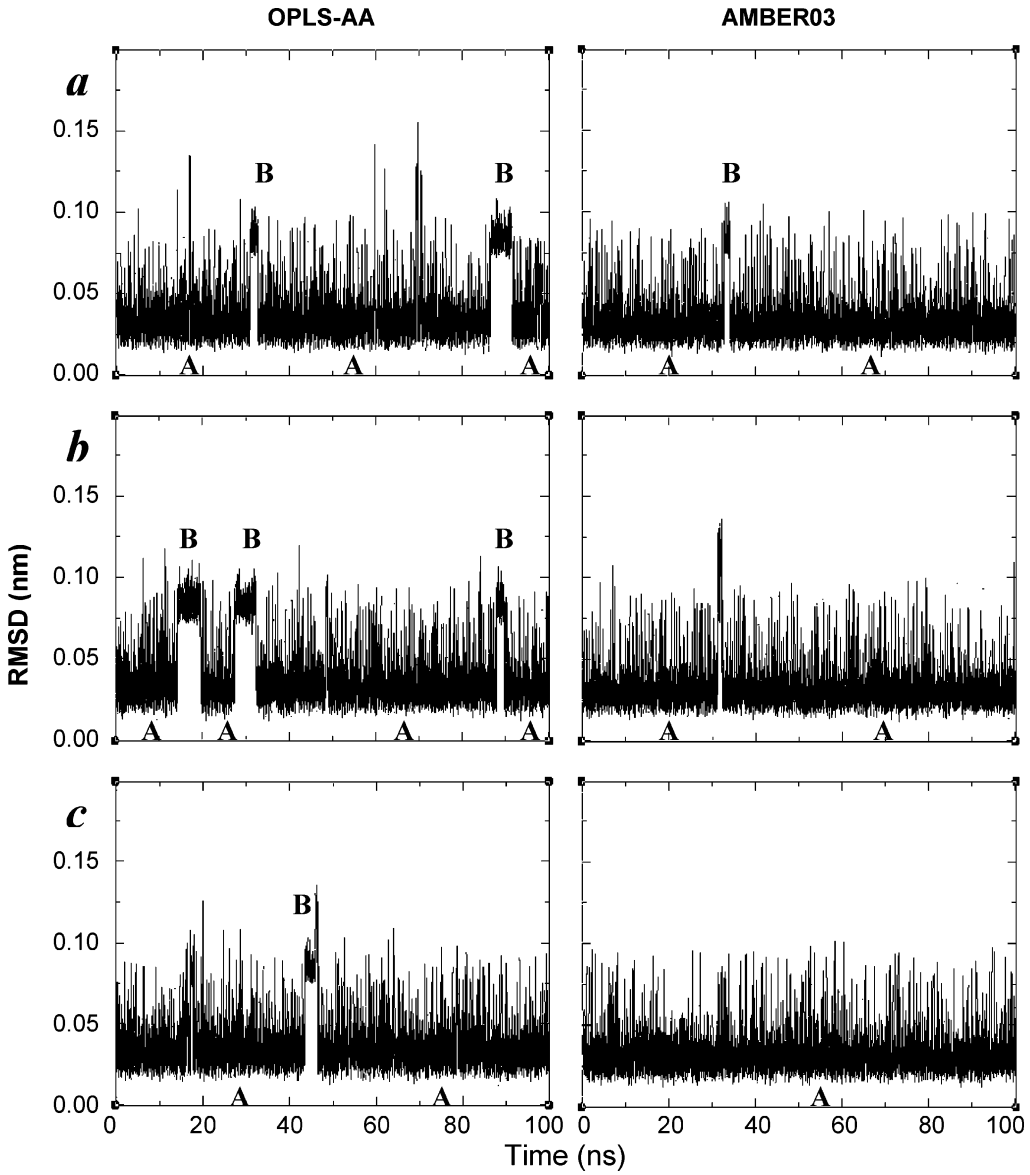

Figure 1. MD trajectories in OPLS-AA force field (left panels) and in AMBER03 force field (right panels) for pA_4 showing root-mean-square deviation values from the initial structure. Panels *a*, *b*, and *c* correspond to runs with different random values for initial velocities. The two different conformational states observed during MD simulation are labeled as A and B.

ϕ and ψ angles were considered, and the ω angles of the amide bonds were allowed to rotate (see Table S1 in Supporting Information). Initial simulations were run for 20 ns for each of the 10 starting structures. For the OPLS-AA force field, simulations converged to the same (or very similar) single predominant structure in six cases, and in the other four cases, simulations showed transitions between two structures, one of them being the same conformer as the observed predominant structure (data not shown). For the AMBER03 force field, similar results were observed. Additional simulations run for 20 ns for three starting structures obtained by a conformational search using the TINKER package available on the Internet (http://dasher.wustl.edu/tinker/) revealed the same general pattern (see structures 11−13 in Table S1). To analyze conformational equilibrium in pA_4 further, three long MD runs of 100 ns starting from different velocities (randomly generated by GROMACS) were performed for one of the starting conformations where the short run of 20 ns did not show any conformational transitions. The long runs for the OPLS-AA force field (Figure 1, left panels) clearly showed conformational transitions between the same two structures as those found previously in short runs. Additionally, three additional 100 ns MD simulations were carried out with the AMBER03 force field using the same starting structure. The predominant conformer A and minor conformer B were also sampled during these MD simulations, which agreed with results obtained using the OPLS-AA force field (Figure 1, right panels). It should also be noted that MD trajectories in Figure 1 occasionally featured some narrow peaks corresponding to conformers different from both A and B; because populations of those conformers were very small, they were ignored as insignificant.

According to these MD simulations, the conformational equilibrium of pA_4 in DMSO solution was characterized by transitions between two main conformers determined by the longer MD runs (Figure 1). One of them (conformer A) was a predominant conformer and the other (conformer B) was a minor conformer. Corresponding populations over all trajectories in Figure 1 were about 93% (the OPLS-run trajectories) and about 99.3% (the AMBER03-run trajectories) for conformer A and about 6.7% (OPLS-AA) and about 0.4% (AMBER03) for conformer B. The average values of the dihedral angles for both conformers over trajectories in Figure 1 are listed in Table 1.

Table 1. Dihedral Angles (in Degrees) for Conformers A and B[a]

		conformer A avg angle value ± SD		conformer B avg angle value ± SD	
residue		OPLS-AA	AMBER03	OPLS-AA	AMBER03
D-Pro[1]	ϕ_1	67.8 ± 9.6	62.7 ± 9.2	69.5 ± 8.3	64.5 ± 9.5
	ψ_1	−118.9 ± 13.9	−125.3 ± 11.0	−112.7 ± 15.5	−115.2 ± 13.3
	ω_{12}	176.5 ± 6.2	175.4 ± 6.2	176.4 ± 7.1	177.9 ± 6.8
Ala[2]	ϕ_2	−93.2 ± 17.5	−79.1 ± 12.4	−102.4 ± 23.8	−83.7 ± 19.4
	ψ_2	8.3 ± 19.0	0.6 ± 15.3	0.2 ± 19.1	−18.5 ± 16.2
	ω_{23}	177.3 ± 8.8	178.3 ± 9.2	−179.9 ± 8.8	−177.9 ± 9.1
Ala[3]	ϕ_3	−126.5 ± 22.1	−124.5 ± 21.0	−145.5 ± 16.1	−153.8 ± 21.3
	ψ_3	−119.3 ± 31.8	−127.7 ± 22.1	74.5 ± 28.2	102.0 ± 40.3
	ω_{34}	173.2 ± 7.4	171.9 ± 7.5	−176.9 ± 6.7	−171.9 ± 9.5
Ala[4]	ϕ_4	−85.9 ± 32.9	−74.7 ± 23.8	81.2 ± 9.3	75.5 ± 30.8
	ψ_4	−32.2 ± 14.6	−30.0 ± 13.2	−48.9 ± 15.5	−47.0 ± 12.3
	ω_{45}	159.0 ± 7.8	155.6 ± 8.4	159.3 ± 7.8	160.3 ± 9.6
Ala[5]	ϕ_5	−114.7 ± 20.3	−117.9 ± 18.8	−111.5 ± 23.3	−128.2 ± 25.5
	ψ_5	145.1 ± 11.4	149.6 ± 9.8	137.1 ± 13.7	147.0 ± 12.6
	ω_{51}	−179.3 ± 8.0	−177.3 ± 8.6	−176.5 ± 7.8	−175.7 ± 8.6

[a] Using the OPLS-AA and AMBER03 force fields averaged over long MD trajectories (Figure 1).

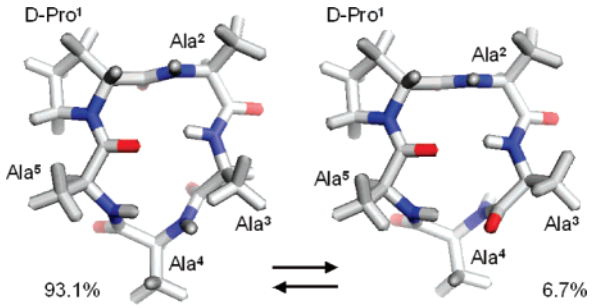

Figure 2. Average structures representing the two conformational states of pA_4, A left) and B (right), which were in equilibrium during 100 ns MD simulation using the OPLS-AA force field. Conformer A does not feature a γ-turn-like conformation for Ala[4], while conformer B does.

One can see that the predominant conformer A does not include any γ-turn-like conformation for the L-amino acid residues, whereas the minor conformer B contains this local conformation for Ala.[4] Both conformers feature the distinct β-II′ turn at D-Pro[1]-Ala[2] stabilized with the hydrogen bond Ala[3]NH···OCAla[5], with the average N···O distance of 3.18 Å and the average value of NH···O angle of 151.6° (conformer A; the corresponding values for conformer B were 3.20 Å and 165.5°). The γ-turn at Ala[4] in conformer B was stabilized with the hydrogen bond Ala[5]NH···OCAla[3], with the average N···O distance of 3.05 Å and the average value of NH···O angle of 156.3°. At the same time, the average number of the peptide NH groups involved in hydrogen bonds with the SO groups of DMSO along the MD trajectory was 2.14 ± 0.72, which agrees with the notion that the NH groups of Ala,[2] Ala[4], and Ala[5] interacted with DMSO most of the time. Geometrically, the difference between the two conformers is mostly in orientation of the peptide bond between residues Ala[3] and Ala[4] (see Figure 2). Conformational states A and B observed with the AMBER03 force field possessed very similar structures. In this case, the population of conformer B featuring a γ-turn-like conformation was significantly lower than for that obtained with the OPLS-AA force field.

The longer MD runs in Figure 1 generated average atom−atom distances in excellent agreement with the 20 experimental proton−proton distances estimated for pA_4 in DMSO solution by measuring NOEs.[4] Table 2 lists these data together with the same calculated distances averaged over the trajectories in Figure 1, as well as over fragments of the trajectories corresponding to conformers A and B separately. Averaging over the entire trajectory exactly fit all 20 experimental distances. For predominant conformer A, no distance was beyond the measured limits for MD runs with both OPLS-AA and AMBER03 force fields. For the minor conformer B (OPLS-AA force field), two distances significantly differed from the experimental limits, namely, αH_4-NH_4 (2.20 ± 0.11 Å vs limits from 2.46 Å to 2.98 Å) and NH_4-NH_5 (3.32 ± 0.31 Å vs limits from 2.24 Å to 2.72 Å). It is noteworthy that the differences in proton−proton distances αH_3-NH_4, αH_4-NH_4, and NH_4-NH_5 are especially indicative of the differences between conformers A and B, while distances $N_3-C'_5$ and C'_3-N_5 are almost the same in both conformers (4.04 ± 0.16 Å and 4.08 ± 0.17 Å for $N_3-C'_5$ and 3.44 ± 0.28 Å and 3.21 ± 0.13 Å for C'_3-N_5 in conformers A and B, respectively). Slightly different from the conformer obtained with the OPLS-AA force field, minor conformer B obtained with the AMBER03 force field had four distances that significantly differed from the experimental limits, namely, αH_2-NH_3 (3.46 ± 0.15 Å vs limits from 2.58 Å to 3.12 Å), αH_3-NH_4 (2.16 ± 0.15 Å vs limits from 2.58 Å to 3.12 Å), αH_4-NH_4 (2.23 ± 0.07 Å vs limits from 2.46 Å to 2.98 Å), and NH_4-NH_5 (3.47 ± 0.21 Å vs limits from 2.24 Å to 2.72 Å).

The predominant conformer A, which featured negative values for both ϕ and ψ for Ala,[4] was somewhat similar to one of the conformers suggested for pA_4 by our previous calculations (see conformer 1 in Table 2[6]). It was not similar, however, to the structure previously proposed as the one with the highest statistical weight in solution.[6] The negative values of ϕ_4 and ψ_4 were also characteristic for one of the conformers of pA_4 suggested earlier by introducing the experimental NMR parameters as constraints in MD simulations (conformer III[4]). The minor conformer B was not found by our previous calculations; at the same time, similar conformers were represented among structures (conformers I and II) suggested by Mierke et al.[4]

Several conclusions can be derived from the results of this study. First, the model CPP, pA_4, is indeed limited in its conformational flexibility, because unconstrained MD runs starting from very different initial structures all converged to the same two conformers shown in Figure 2. Second, our results clearly showed that averaging over the long unrestricted MD run yielded excellent agreement with available experimental NMR parameters. These results support the general validity of averaging over low-energy conformations independently obtained by energy calculations for CPPs in solution, proposed in our previous study.[6] Third, the results on the conformational flexibility of pA_4 were quite similar in MD runs using either

Table 2. Proton−Proton Distances in Å ± SD[a]

interproton contact[b]	exptl limits		total trajectories		conformer A		conformer B	
	lower	upper	OPLS-AA	AMBER03	OPLS-AA	AMBER03	OPLS-AA	AMBER03
ProH$^{\alpha}$−Ala^{2}NH	2.00	2.37	2.19 ± 0.13	2.18 ± 0.12	2.20 ± 0.13	2.18 ± 0.12	2.21 ± 0.14	2.20 ± 0.12
ProH$^{\alpha}$−Ala^{3}NH	3.28	3.97	3.63 ± 0.25	3.57 ± 0.23	3.63 ± 0.26	3.57 ± 0.23	3.67 ± 0.25	3.57 ± 0.23
Proqδ_2−Ala^{5}NH	3.61	4.87	4.79 ± 0.15	4.87 ± 0.13	4.81 ± 0.15	4.87 ± 0.12	4.75 ± 0.14	4.79 ± 0.13
Proqδ_2−Ala^{5}H$^{\alpha}$	2.11	3.05	2.65 ± 0.11	2.67 ± 0.12	2.66 ± 0.11	2.67 ± 0.12	2.64 ± 0.11	2.68 ± 0.15
Proqδ_2−Ala^{5}qβ_3	2.65	4.60	3.74 ± 0.22	3.63 ± 0.18	3.72 ± 0.21	3.62 ± 0.17	3.84 ± 0.24	3.66 ± 0.21
Ala^{2}NH−Ala^{2}H$^{\alpha}$	2.71	2.98	2.95 ± 0.08	2.92 ± 0.08	2.95 ± 0.08	2.92 ± 0.08	2.95 ± 0.08	2.93 ± 0.09
Ala^{2}NH−Ala^{2}qβ_3	2.56	3.12	2.60 ± 0.17	2.53 ± 0.11	2.59 ± 0.16	2.53 ± 0.11	2.79 ± 0.06	2.56 ± 0.15
Ala^{2}NH−Ala^{3}NH	2.30	2.78	2.58 ± 0.37	2.77 ± 0.29	2.60 ± 0.36	2.77 ± 0.29	2.42 ± 0.33	2.58 ± 0.30
Ala^{2}H$^{\alpha}$−Ala^{3}NH	2.58	3.12	3.22 ± 0.24	3.26 ± 0.20	3.20 ± 0.25	3.25 ± 0.20	3.28 ± 0.23	**3.46** ± 0.15
Ala^{2}qβ_3−Ala^{3}NH	2.76	3.83	3.74 ± 0.22	3.74 ± 0.18	3.75 ± 0.21	3.74 ± 0.18	3.71 ± 0.25	3.51 ± 0.23
Ala^{3}H$^{\alpha}$−Ala^{3}NH	2.44	2.96	2.94 ± 0.09	2.96 ± 0.07	2.94 ± 0.08	2.96 ± 0.07	2.92 ± 0.09	2.91 ± 0.08
Ala^{3}H$^{\alpha}$−Ala^{4}NH	2.58	3.12	3.15 ± 0.38	3.22 ± 0.22	3.29 ± 0.21	3.24 ± 0.18	2.41 ± 0.26	**2.16** ± 0.15
Ala^{3}NH−Ala^{3}qβ_3	2.66	3.52	2.90 ± 0.21	2.84 ± 0.18	2.88 ± 0.21	2.84 ± 0.18	3.01 ± 0.17	3.07 ± 0.17
Ala^{3}NH−Ala^{5}NH	3.46	4.19	3.58 ± 0.41	3.63 ± 0.38	3.61 ± 0.40	3.64 ± 0.38	3.33 ± 0.36	3.25 ± 0.30
Ala^{4}NH−Ala^{4}H$^{\alpha}$	2.46	2.98	2.82 ± 0.28	2.90 ± 0.12	2.92 ± 0.12	2.91 ± 0.09	**2.20** ± 0.11	**2.23** ± 0.07
Ala^{4}NH−Ala^{5}NH	2.24	2.72	2.49 ± 0.46	2.53 ± 0.29	2.34 ± 0.30	2.51 ± 0.27	**3.32** ± 0.31	**3.47** ± 0.21
Ala^{4}H$^{\alpha}$−Ala^{5}NH	3.02	3.64	3.49 ± 0.12	3.49 ± 0.12	3.49 ± 0.12	3.49 ± 0.11	3.47 ± 0.11	3.52 ± 0.10
Ala^{4}qβ_3−Ala^{5}NH	2.61	3.66	3.17 ± 0.23	3.25 ± 0.22	3.18 ± 0.23	3.25 ± 0.22	3.16 ± 0.25	3.24 ± 0.22
Ala^{5}NH−Ala^{5}H$^{\alpha}$	2.64	2.98	2.94 ± 0.08	2.95 ± 0.07	2.94 ± 0.08	2.95 ± 0.07	2.94 ± 0.09	2.92 ± 0.08
Ala^{5}NH−Ala^{5}qβ_3	2.65	3.54	2.80 ± 0.19	2.84 ± 0.16	2.80 ± 0.19	2.84 ± 0.15	2.79 ± 0.20	2.94 ± 0.16

[a] Calculated by averaging over trajectories of the 100 ns MD simulations and over two conformational states separately. Experimental measurements taken from Mierke et al.[3] Calculated average distances outside experimental range shown in bold. [b] q represents pseudoatoms (i.e., the corresponding C$^{\beta}$ or C$^{\delta}$ atoms).

the OPLS-AA or AMBER03 force fields (see Figure 1) showing independence of the force field utilized. Some other specifics of calculation protocols utilized may be more important. For instance, elaborated free-energy calculations applied to pA$_4$ by others yielded several conformers that violated at least 5 out of the 20 experimental proton−proton distances.[13]

Our results showed that the γ-turn-like conformation for Ala^4 was present only in the minor conformer B of pA$_4$, consistent with the rare occurrence of this specific type of conformation for L-amino acid residues in CPPs in available experimental data.[2,7] In fact, conformer A alone fully satisfied the experimental data of NOE measurements,[4] as shown in Table 2. Conformers A and B deduced in this study were very close to the two main conformers suggested very recently by Heller et al. that re-examined the conformational flexibility of pA$_4$.[8] At the same time, this study does not support the assertion that the population of the γ-turn-containing conformer in DMSO could be estimated as high as 15−30%.[8] The authors reached that conclusion based primarily on qualitative estimations of ^{13}C′−^{1}H^{N} cross-peak volumes in long-range HNCO experiments and by MD simulations (40 ns) that employed a protocol identical to that used in this study.[8] However, they may have used the OPLS-AA parameters for DMSO molecules in GROMACS[9] that do not reflect correctly the bulk properties of DMSO (density = 1067 kg/m^3 and ΔH_{vap} = 42.2 kJ/mol, the experimental values being 1095 kg/m^3 and 52.88 kJ/mol, respectively,[10] as resulted from our additional calculations using these parameters, which fully reproduced the results of MD simulations by Heller et al.[8]). It should also be noted that our calculations may, in fact, overestimate the population of conformer B in solution, because force fields employing flexible valence geometry generally tend to overestimate the population of the Ramachandran map region with positive ϕ and negative ψ values for L-amino acid residues.[14] On the other hand, conformers of CPPs similar to conformer B may easily become predominant for CPPs that replace Ala^4 with glycine, because there are no steric limitations on the γ-turn-like conformations for glycine.[15]

Finally, our study established that the conformational flexibility of pA$_4$ in DMSO solution is almost exclusively limited to a specific conformer (conformer A). This conformer may be used as a conformational template mimicking, to some extent, different types of β-turns. Specifically, the ϕ,ψ values in Table 1 suggest that the peptide chain reversal at the D-Pro^1-Ala^2 residues is somewhat close to the β-II′ turn (the standard ϕ,ψ values are 60°, −120°; −80°, 0°), and the one at Ala^5-D-Pro^1 may be assigned to the β-V-like turn (the standard ϕ,ψ values are −80°, 80°; 80°, −80°; the standard values for the β-turns from Rose et al.[16]). On the other hand, the conformation of Ala^4 is close to that of the 3/10 helix (the standard ϕ,ψ values were suggested as −57° and −30°[17]).

Acknowledgment. This work has been supported in part by the NIH GM 68460 grant.

Supporting Information Available: Table S1 lists dihedral angles of 13 starting structures of pA$_4$ and Table S2 lists atomic coordinates (the PDB format) of the averaged structures A and B obtained by employing the OPLS-AA force field. This material is available free of charge via the Internet at http://pubs.acs.org.

References

(1) Tyndall, J. D.; Pfeiffer, B.; Abbenante, G.; Fairlie, D. P. Over one hundred peptide-activated G protein-coupled receptors recognize ligands with turn structure. *Chem. Rev.* **2005**, *105*, 793−826.
(2) Viles, J. H.; Mitchell, J. B.; Gough, S. L.; Doyle, P. M.; Harris, C. J.; Sadler, P. J.; Thornton, J. M. Multiple solution conformations of the integrin-binding cyclic pentapeptide *cyclo*(-Ser-D-Leu-Asp-Val-Pro-). Analysis of the (phi, psi) space available to cyclic pentapeptides. *Eur. J. Biochem.* **1996**, *242*, 352−362.
(3) Kessler, H.; Gratias, R.; Hessler, G.; Gurrath, M.; Müller, G. Conformation of cyclic peptides. Principle concepts and the design of selectivity and superactivity in bioactive sequences by "spatial screening". *Pure Appl. Chem.* **1996**, *68*, 1201−1205.
(4) Mierke, D. F.; Kurz, M.; Kessler, H. Peptide flexibility and calculations of an ensemble of molecules. *J. Am. Chem. Soc.* **1994**, *116*, 1042−1049.
(5) Nemethy, G.; Printz, M. P. The γ turn, a possible folded conformation of the polypeptide chain. Comparison with the β turn. *Macromolecules* **1972**, *6*, 755−758.
(6) Nikiforovich, G. V.; Kövér, K. E.; Zhang, W. J.; Marshall, G. R. Cyclopentapeptides as flexible conformational templates. *J. Am. Chem. Soc.* **2000**, *122*, 3262−3273.

(7) Fuji, N.; Oishi, S.; Hiramatsu, K.; Araki, T.; Ueda, S.; Tamamura, H.; Otaka, A.; Kusano, S.; Terakubo, S.; Nakashima, H.; Broach, J. A.; Trent, J. O.; Wang, Z. X.; Peiper, S. C. Molecular-size reduction of a potent CXCR4-chemokine antagonist using orthogonal combination of conformation- and sequence-based libraries. *Angew. Chem., Int. Ed.* **2003**, *42*, 3251−3253.
(8) Heller, M.; Sukopp, M.; Tsomaia, N.; John, M.; Mierke, D. F.; Reif, B.; Kessler, H. The conformation of *cyclo*(-D-Pro-Ala_4-) as a model for cyclic pentapeptides of the DL_4 type. *J. Am. Chem. Soc.* **2006**, *128*, 13806−13814.
(9) Lindahl, E.; Hess, B.; Van der Spoel, D. GROMACS 3.0: A package for molecular simulation and trajectory analysis. *J. Mol. Mod.* **2001**, *7*, 306−317.
(10) Zheng, Y.-J.; Ornstein, R. L. A molecular dynamics and quantum mechanics analysis of the effect of DMSO on enzyme structure and dynamics: Subtilisin. *J. Am. Chem. Soc.* **1996**, *118*, 4175−4180.
(11) Riddick, J. A.; Bunger, W. B.; Sakand, T. K. *Organic solvents: Physical Properties and Methods of Purification*; John Wiley and Sons: New York, 1986.
(12) Berendsen, H. J. C.; Postma, J. P. M.; van Gunsteren, W. F.; DiNola, A.; Haak, J. R. Molecular dynamics with coupling to an external bath. *J. Chem. Phys.* **1984**, *81*, 3684−3690.
(13) Baysal, C.; Meirovitch, H. Ab initio prediction of the solution structures and populations of a cyclic pentapeptide in DMSO based on an implicit solvation model. *Biopolymers* **2000**, *53*, 423−433.
(14) Rodriguez, A. M.; Baldoni, H. A.; Suvire, F.; Vázquez, R. N.; Zamarbide, G.; Enriz, R. D.; Farkas, Ö.; Perczel, A.; McAllister, M. A.; Torday, L. L.; Papp, J. G.; Csizmadia, I. G. Characteristics of Ramachandran maps of L-alanine diamides as computed by various molecular mechanics, semiempirical and ab initio MO methods: A search for primary standard of peptide conformational stability. *J. Mol. Struct.: THEOCHEM* **1998**, *455*, 275−301.
(15) Dechantsreiter, M. A.; Planker, E.; Matha, B.; Lohof, E.; Holzemann, G.; Jonczyk, A.; Goodman, S. L.; Kessler, H. N-Methylated cyclic RGD peptides as highly active and selective alpha(V)beta(3) integrin antagonists. *J. Med. Chem.* **1999**, *42*, 3033−3040.
(16) Rose, G. D.; Gierarsch, L. M.; Smith, J. A. Turns in peptides and proteins. *Adv. Protein Chem.* **1985**, *37*, 1−109.
(17) Toniolo, C.; Benedetti, E. The polypeptide 310-helix. *Trends Biochem. Sci.* **1991**, *16*, 350−353.

JM070084N